

Nonlinear Oscillations and Chaos in Electrical Breakdown in Ge

S. W. Teitsworth and R. M. Westervelt

Division of Applied Sciences and Department of Physics, Harvard University, Cambridge, Massachusetts 02138

and

E. E. Haller

Lawrence Berkeley Laboratory, Berkeley, California 94720

(Received 16 June 1983)

Self-generated nonlinear oscillations and chaos are found in the conductance of liquid-He-cooled far-infrared photoconductors made from ultrapure Ge. Complex behavior includes a period-doubling cascade to chaotic oscillation with increasing applied electric field, quasiperiodic oscillation, frequency locking, and intermittent switching between modes of oscillation. A rate-equation model is presented which includes impurity impact ionization and space-charge injection.

PACS numbers: 72.70.+m, 05.40.+j, 05.70.Ln

The performance of many semiconductor devices is limited by the onset of instabilities or breakdown at high electric fields. Recent advances in the theory of nonlinear dynamical systems¹⁻³ have been successfully tested⁴⁻⁶ in a number of important experimental systems drawn from hydrodynamics, chemical reaction kinetics, lasers, Josephson junctions,^{5,6} and driven diode circuits.⁴ However, relatively little work has been reported for semiconductor devices.⁷ The examination of semiconductor instabilities⁸ from this new perspective should provide a deeper understanding of the operation of practical semiconductor devices in nonlinear regimes.

We report here the observation of nonlinear oscillatory instabilities and chaotic behavior due to impurity impact ionization in cooled extrinsic far-infrared (FIR) Ge photoconductors^{9,10} with shallow acceptor concentrations $a \sim 10^{10}$ to 10^{13} cm⁻³. These devices provide useful models for the noise performance of doped extrinsic Ge FIR photoconductors with $a \sim 10^{14}$ to 10^{15} cm⁻³, made in an identical manner, which are among the most sensitive detectors in this wavelength region. In addition to oscillatory instabilities, we find that the conductance of ultrapure Ge devices exhibits complex behavior including the period-doubling route to chaos, quasiperiodic oscillations, frequency locking, and intermittent switching between different modes of oscillation; all of which can be important sources of spectrally sharp and broadband noise.

We studied eighteen devices from four different crystals of *p*-type ultrapure Ge, fabricated at Lawrence Berkeley Laboratory,¹⁰ with the following characteristics: crystal 463, $a \sim 2.5 \times 10^{10}$ cm⁻³, dislocated, conduction along $\langle 100 \rangle$; crystal

150, $a \sim 10^{11}$ cm⁻³, dislocation free, $\langle 110 \rangle$; crystal 295, $a \sim 2 \times 10^{11}$ cm⁻³, dislocation free, $\langle 110 \rangle$; and crystal 374, $a \sim 10^{12}$ cm⁻³, dislocated, $\langle 100 \rangle$. Dislocated crystals have shallow (10–11 meV) acceptor levels due to B or Ga impurities while undischarged crystals have deep (72 meV) levels due to divacancy-hydrogen complexes¹⁰ in addition. The compensation ratio is estimated to be $d/a \sim 0.1$ to 1, where d is the donor concentration. Samples were cut to sizes $0.5 \times 0.5 \times 8$ mm³ to roughly $20 \times 20 \times 8$ mm³ and electrical contacts made with use of B-ion-implanted p^+ layers which remain metallic at liquid He temperatures. Two or more contacts were fabricated either on opposing faces or along one side of each sample.

Electrical measurements were made at temperatures from $T = 1.5$ to 4.2 K at which few impurities are thermally ionized. External visible and FIR radiation were excluded by cold metal shields. A blackbody radiator with adjustable temperature ≤ 30 K located inside the shield served as a time-independent source of FIR radiation, which determined the hole concentration, typically $p \sim 10^3$ to 10^7 cm⁻³. The dc current-voltage (I - V) curves for each sample were measured under constant applied voltage or constant current. In both cases the dc I - V curves were identical, with no hysteresis or reentrant regions, and had the following characteristics, typical of FIR photoconductors⁹: at low average fields $E < 0.5$ V/cm the I - V curves were linear (we define $E = V/L$ with L the contact separation), and for moderate fields 0.5 V/cm $< E < E_b$, $I \propto V^p$ where $p \sim 2$; the magnitude of I in both cases scaled with FIR illumination intensity. At a critical average field $E_b \sim 3$ to 40 V/cm depending on sample characteristics, the current abruptly increased by several orders of magni-

tude as a result of impact ionization¹¹ of shallow impurity levels in the entire sample.

Above a well-defined threshold average dc field $E_t < E_b$ the conductance $G(t) = I(t)/V(t)$ for constant FIR illumination becomes time dependent, and with increasing field E a series of progressively more complex oscillatory instabilities is observed at low frequencies $f < 10$ kHz. For average fields $E < E_b$ the local field $E(x)$ can exceed the breakdown value E_b as a result of spatial inhomogeneity produced by contact geometry, FIR illumination, or space-charge injection, causing instability. The character of these instabilities is very similar for both dc current and dc voltage bias, and is essentially independent of the external circuit and type of current or voltage bias. The patterns of instabilities found in a given sample varied with contact geometry and FIR illumination as described below.

A particularly clear example of a period-doubling cascade into chaotic oscillations¹⁻³ is shown in the data of Figs. 1 to 3 for crystal 463. The current $I(t)$ and phase portrait are plotted in Figs. 1(a) to 1(d) for dc voltage bias with a series of increasing average dc fields $E > E_t$. In Fig. 1(a) the instability appears to be a simple periodic oscillation accompanied by instrumental noise. As the applied field increases the symmetry of oscillation changes to a period-doubled form as shown in Fig. 1(b), and to period four in Fig. 1(c). At a

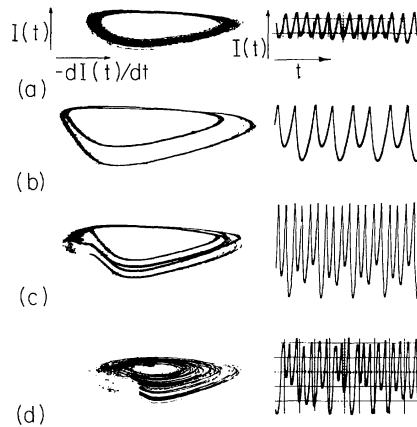


FIG. 1. Oscillatory current $I(t)$ and phase portrait, $I(t)$ vs $dI(t)/dt$, for Ge sample 463A at $T = 4.2$ K with increasing applied voltage V from (a) to (d) (see Fig. 2); $I(t)$ scale/div (a) 1 nA, 2 msec; (b) 5 nA, 2 msec; (c) 5 nA, 5 msec; (d) 10 nA, 5 msec. Sample geometry $0.4 \times 1 \times 8$ mm³, two B-implanted p^+ contacts 1.0×1.8 mm² at opposite ends of one 1×8 mm² face.

larger dc field E well below the breakdown field E_b the oscillation in $I(t)$ becomes chaotic as shown in Fig. 1(d); the current trace $I(t)$ remains oscillatory in appearance but no longer repeats itself, and the phase portrait forms a broad band. This chaotic oscillation is clearly distinct from the low-level broadband current noise which accompanies breakdown of the entire sample at higher applied fields $E > E_b$.

The experimental bifurcation diagram for this sequence of instabilities is shown in Fig. 2. This diagram was produced by electronically plotting the observed minima of $I(t)$ (see Fig. 1) along the vertical axis while sweeping the applied voltage, plotted along the horizontal axis. The transitions from simply periodic to period-two and period-four regimes of oscillation are evident in Fig. 2 as well as a broad region of chaotic oscillation. This diagram is similar in some respects to that computed for a quadratic one-dimensional map.² From Fig. 2 and similar bifurcation diagrams we obtain estimates of the scaling parameters,³ $\alpha \approx 1.5$ and $\delta \approx 2.7$, to be compared with theory,³ $\alpha = 2.50$ and $\delta = 4.67$. We do not expect close agreement, because we observe only two period doublings, and because the experimental map may have dimension > 1 .

A series of power spectra $S(f)$ computed from records of the current $I(t)$ under the same conditions as Figs. 1 and 2 are shown in Figs. 3(a) to 3(e). Comparing 3(a) and 3(b) we find a period-3 to period-2 transition of the frequency-locking type rather than a simple period doubling. Period 4 occurs in the conventional manner as shown in Fig. 3(c). From these and similar data we compute the average spectral power ratio¹² $2\beta^{(2)} \approx 14$ dB in good agreement with the theoretical¹² value $2\beta^{(2)} = 13.2$ dB for the quadratic one-dimensional map. The onset of chaos appears in spec-

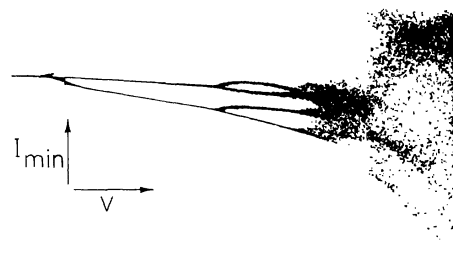


FIG. 2. Bifurcation diagram of current minima I_{\min} vs applied voltage V for sample 463A at $T = 4.2$ K, for range $V = 11.1$ to 18.4 V; breakdown of the entire sample occurred at $V_b = 20$ V.

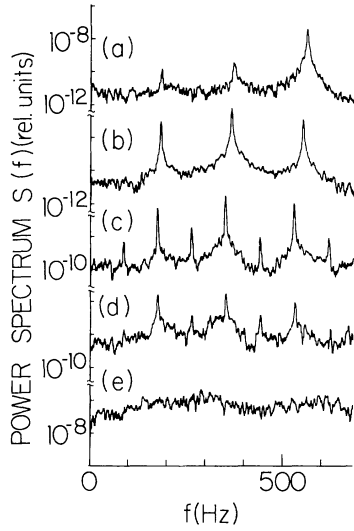


FIG. 3. Power spectra $S(f)$ computed from $I(t)$ for sample 463A at $T=4.2$ K with applied voltage increasing from (a) to (e) (see Fig. 2).

tra Figs. 3(d) and 3(e) primarily as a rising level of broadband noise which eventually covers the sharp peaks due to periodic oscillation; note the absence of low-frequency noise of the form $S(f) \propto f^{-p}$, $p \sim 1$.

The performance of doped extrinsic photoconductors is typically limited by noise at frequencies below 10 Hz. From Fig. 3 and power spectra data on many other Ge samples we find a hierarchy of noise sources: The periodic oscillatory instability, Figs. 3(a) to 3(c), is not associated with excess broadband noise; chaos, Figs. 3(d) and 3(e), produces moderate levels of broadband noise spectrally flat at low frequencies; and intermittent switching between modes of oscillation (e.g., period 3 and period 4) produces large levels of low-frequency noise¹³ near $f \sim 1$ Hz, when present (see below).

The majority of Ge samples studied displayed complex behavior, which often took the form of coupled nonlinear oscillations. Period doubling followed by chaos was observed in twelve of eighteen samples, taken from all four crystals; quasi-periodic oscillation at two incommensurate frequencies was found in four samples; evidence of frequency locking was found in six samples; and intermittent switching between different modes of oscillation was found in three samples. All Ge samples studied displayed a simple oscillatory instability above a threshold average dc field E_t . For low FIR illumination intensity ($p < 10^6$ cm⁻³)

the conductance $G(t)$ developed periodic sharp spikes; the frequency of this relaxation oscillation increased with FIR illumination from values $f_0 < 10^{-1}$ Hz to $f_0 \sim 10^2$ Hz. For moderate FIR illumination intensity ($p \sim 10^6$ cm⁻³) the conductance developed a smooth periodic oscillation with frequency $f_0 \sim 10^2$ to 10^4 Hz as shown in Fig. 1(a); for large E the excursion in $G(t)$ became quite large and approached the average value. These instabilities are similar to spiking and oscillatory transients (hook anomaly) which limit the performance of extrinsic photoconductors.⁹

We propose the following rate-equation model¹⁴ as a physical explanation for the oscillatory instabilities described above. This model is based on impact ionization of charge stored on shallow acceptor levels, and space-charge injection.¹⁵ For a one-dimensional sample geometry, the concentrations of holes $p(x,t)$ and ionized acceptors $a_*(x,t)$, and the local electric field $E(x,t)$ are given by (neglecting diffusion terms for simplicity)

$$\partial a_*/\partial t = \gamma(a - a_*) + p\kappa(a - a_*) - pra_*, \quad (1)$$

$$\begin{aligned} \partial p/\partial t + (\mu E)\partial p/\partial x \\ = \partial a_*/\partial t - (e\mu/\epsilon)p(p + d - a_*), \end{aligned} \quad (2)$$

$$\partial E/\partial t = J_{\text{ext}}/\epsilon - (e\mu/\epsilon)pE. \quad (3)$$

In Eq. (1) γ determines the hole generation rate, and $\kappa(E)$ and $r(E)$ the rates of impact ionization and recombination^{11, 16}; a and d are the concentrations of shallow acceptors and donors. Hole flow and space-charge injection are determined by Eq. (2) where μ is the mobility and ϵ the dielectric constant. Equation (3) describes the displacement current in Maxwell's equations, with J_{ext} the external current density.

Without injected space charge Eqs. (1) to (3) have a spatially uniform solution for which $p(t) = a_*(t) - d$, and Eq. (2) reduces to Eq. (1). Linear stability analysis of Eqs. (2) and (3) about steady-state values p_0 and E_0 yields an oscillatory instability with frequency $f_0^2 \simeq e\mu E_0 p_0 a (d\kappa/dE)_{E_0} / 4\pi^2 \epsilon$ when the local field $E(x) > E_b$, because of the inductive nature of the impurity discharge. Under our experimental conditions we calculate $f_0 \sim 10$ kHz, and we propose that the fast smooth oscillations in our samples are produced by this mechanism in spatially localized high-field regions.

At low temperatures and low FIR illumination, the quantity of space charge in the form of excess holes injected into the sample and trapped on ionized acceptors typically exceeds the total

charge associated with free holes.¹⁶ Dielectric relaxation determines the spatial distribution of trapped space charge, which accumulates very near the injecting contact.¹⁶ By decreasing a_* in Eq. (1), trapped space charge can shift the breakdown field E_b to lower values,¹¹ producing a relaxation oscillation. As a_* approaches zero, $\partial a_*/\partial t$ becomes positive [Eq. (1)] and an impurity discharge occurs. This process repeats with a period determined by the time to reload the acceptors, $\sim 1/p_0 r \sim 0.01$ to 100 sec under our experimental conditions, in agreement with the periodic spiking we observe. Complex instabilities are produced in many physical systems¹ by the interaction of two or more nonlinear modes of oscillation. In our system these can be slow relaxation and smooth modes of oscillation of a single spatially localized discharge, or of two or more separated discharges. Analytic and numerical work on simplified spatial models for Eqs. (1) to (3) is in progress.¹⁴

We thank P. C. Martin for useful discussions. This work was supported in part by the Research Corporation, and the U. S. Office of Naval Research through Grant No. N00014-75-C-0648. One of us (S.W.T.) acknowledges receipt of a Robert L. Wallace Fellowship.

¹R. H. G. Helleman, in *Fundamental Problems in Statistical Mechanics V*, edited by E. G. D. Cohen (North-Holland, Amsterdam, 1980), p. 165, and ref-

erences therein.

²P. Collet and J.-P. Eckmann, *Iterated Maps on the Interval as Dynamical Systems* (Birkhauser, Boston, 1980).

³M. J. Feigenbaum, *J. Stat. Phys.* **19**, 25 (1978).

⁴J. Testa, J. Perez, and C. D. Jeffries, *Phys. Rev. Lett.* **48**, 714 (1982).

⁵D. D'Humieres, M. R. Beasley, B. A. Huberman, and A. Libchaber, *Phys. Rev. B* **26**, 3483 (1982).

⁶R. F. Miracky, J. Clarke, and R. H. Koch, *Phys. Rev. Lett.* **50**, 856 (1983).

⁷K. Aoki, K. Miyame, T. Kobayashi, and K. Yamamoto, *Physica (Utrecht)* **117&118B**, 570 (1983).

⁸H. Hartnagel, *Semiconductor Plasma Instabilities* (American Elsevier, New York, 1969).

⁹P. R. Bratt, in *Semiconductors and Semimetals*, edited by R. K. Willardson and A. C. Beer (Academic, New York, 1977), p. 39.

¹⁰E. E. Haller, W. L. Hansen, and F. S. Goulding, *Adv. Phys.* **30**, 93 (1981).

¹¹L. M. Lambert, *J. Phys. Chem. Solids* **23**, 1481 (1962).

¹²M. Nauenberg and J. Rudnick, *Phys. Rev. B* **24**, 493 (1981).

¹³F. T. Arecchi and F. Lisi, *Phys. Rev. Lett.* **49**, 94 (1982); not $1/f$ noise as noted by M. R. Beasley, D. D'Humieres, and B. A. Huberman, *Phys. Rev. Lett.* **50**, 1328 (1983); and R. F. Voss, *Phys. Rev. Lett.* **50**, 1329 (1983).

¹⁴S. W. Teitworth and R. M. Westervelt, to be published.

¹⁵Negative-differential-mobility effects are ruled out by the small values of the transit time $\sim 1 \mu\text{sec}$ and dielectric relaxation time $\sim 1 \mu\text{sec}$ relative to the period of oscillation $> 0.1 \text{ msec}$ in our samples.

¹⁶A. Rose, *Concepts in Photoconductivity and Allied Problems* (Krieger, Melbourne, Fla., 1978).